one can reduce the output timing jitter significantly by choosing the pre- and post-compensation of residual dispersion judiciously.

Optical pulse propagation in a fiber is governed by the nonlinear Schroedinger (NLS) equation[3]

$$i\frac{\partial A}{\partial z}+\frac{\beta}{2}\frac{\partial^2 A}{\partial t^2}+\gamma|A|^2A=0, \qquad (1)$$

where A is the pulse amplitude, β is the (group-velocity) dispersion coefficient and γ is the nonlinearity coefficient. A typical DM system consists of a pre-compensation fiber, followed by a periodic sequence of anomalous and normal fibers, and a post-compensation fiber. For such a system, Eq. (1) cannot be solved analytically. In the moment method,[4] one defines the pulse energy $E=\int_{-\infty}^{\infty}|A|^2dt$, the time delay $T=\int_{-\infty}^{\infty}t|A|^2dt$ and the frequency $W=(i/2E)\int_{-\infty}^{\infty}(A^*A_t-AA_t^*)dt$, and uses the NLS equation to derive ordinary differential equations for these moments of the pulse amplitude. If one includes the effects of loss and lumped amplification, one finds that the energy is depleted and replenished periodically. The frequency and time shifts evolve according to the equations

$$\frac{dW}{dz}=\sum_{j=1}^{n}W_j\delta(z-z_j),$$
$$\frac{dT}{dz}=\beta W+\sum_{j=1}^{n}T_j\delta(z-z_j), \qquad (2)$$

where W_j and T_j are the (random) frequency and time shifts imposed on the pulse at the jth amplifier, z_j is the position of the jth amplifier and n is the number of stages in the system. Grigoryan *et al.*[2] derived general formulas for the variances of the frequency and time shifts, and their correlation.

Further analysis requires the selection of a specific pulse shape. We used the shape ansatz

$$A=a\exp[i\phi-iW(t-T)-(1+ic)(t-T)^2/2\tau^2], \qquad (3)$$

where the amplitude a, phase ϕ, frequency, time delay, chirp c and width τ are functions of z. By substituting ansatz (3) into the general formulas derived by Grigoryan *et al.*, we obtained specific formulas for the frequency and time shifts, which depend on the amplifier strengths, and the pulse parameters W, T, c and . We solved Eqs. (2) analytically for two cases of interest.

For (moderate-power) DMS pulses one chooses the input power and (dispersion) length of the pre-compensation fiber to balance the average dispersion $\langle\beta\rangle$ of each stage.[5] Consequently, the chirp and width vary periodically with distance, and have the same values at every amplifier. The only free parameter of such a system is the (dispersion) length of the post-compensation fiber. One can reduce, but not eliminate, the output timing jitter if the average-dispersion coefficient has the opposite sign to the dispersion coefficient of the first fiber in each stage.

For (low-power) CRZ pulses, the dependences of the chirp and width on distance are well-approximated by analytical solutions of the linear Schroedinger equation. When the average dispersion is nonzero, the chirp and width have different values at every amplifier. We obtained a formula for the output timing jitter, and its dependence on the amount of pre- and post-compensation. One can minimize the output jitter (cancel the contributions that scale as n^3) by choosing the pre-and post-compensation judiciously. One particular choice also mimimizes the jitter within the system. We derived a formula for this optimal compensation.

In Fig. 1 the standard deviation of the timing jitter is plotted as a function of stage number for a CRZ system with $n = 50$. Each stage consists of an anomalous fiber with $\alpha_a = 0.2$ (dB/Km), $\beta_a = -20.4$ (ps^2/Km) and $l_a = 50$ (Km), and a normal fiber with $\alpha_n = 0.4$, $\beta_n = 102$ and $l_n = 9.9$. For these parameters $\langle\beta\rangle = -0.2$. The pre- and post-compensation fibers have the same loss and dispersion coefficients as the normal fibers, and the pulse full-width at half-maximum is 10 (ps). The solid lines represent our analytical solutions of Eqs. (2) and the dots represent the numerical solutions averaged over 10^4 realizations. The figure shows that our analytical predictions are consistent with numerical solutions of the moment equations, on which they are based. Comparisons of our analytical predictions and numerical solutions of the NLS equation (1) will be described during our presentation.

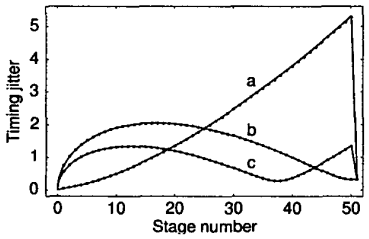

CThL49 Fig. 1 Timing jitter (ps) plotted as a function of stage number for the parameters described in the text. (*a*) No pre-compensation and complete post-compensation. (*b*) Complete pre-compensation and no post-compensation. (*c*) Optimal combination of pre- and post-compensation.

References

1. J.P. Gordon and H.A. Haus, Opt. Lett. **11**, 665 (1986).
2. V S. Grigoryan, C.R. Menyuk and R.M. Mu, J. Lightwave Technol. **17**, 1347 (1999).
3. G.P. Agrawal, *Nonlinear Fiber Optics, 2nd Edition* (Academic, San Diego, 1995).
4. S.N. Vlasov, V.A. Petrishchev and V.I. Talanov, Radiophys. Quantum Electron. **14**, 1353 (1971).
5. T.I. Lakoba, J. Yang, D.J. Kaup and B.A. Malomed, Opt. Commun. **149**, 366 (1998).

CThL50 **1:00 pm**

Influence of chirp on optical free-space communication systems employing preamplified direct detection

Martin M. Strasser,[1] Peter J. Winzer,[2] Martin Pfennigbauer,[1] [1]*Institut für Nachrichtentechnik und Hochfrequenztechnik, Technische Universität Wien, Gusshausstrasse 25/389, A-1040 Wien, Austria; email: strasser@nt.tuwien.ac.at;* [2]*presently at Bell Laboratories, Lucent Technology, Holmdel, NJ 07733, USA*

With the large-scale commercial deployment of Erbium-doped fiber amplifiers, optically preamplified direct detection (DD) receivers have become the technically most practicable way of achieving (nearly) quantum limited receiver performance in the 1.5 μm wavelength range. In *fiber communication* systems, DD reception is affected by chirp due to fiber dispersion and nonlinear effects, but in *free-space communications*, narrow optical filtering changes receiver sensitivity if the input signal is chirped. We present a detailed investigation on the influence of chirp in free-space preamplified DD systems and analyze the (different!) impact in the case of non-return-to-zero (NRZ) and return-to-zero (RZ) coding. Optimizing the optical and electrical receiver bandwidths leads to improved sensitivity.

Commonly, chirp is characterized by a constant *effective* chirp parameter α[1] which defines the derivative of the signal's phase as $d\phi/dt = \frac{1}{2}(\alpha/p)(dp/dt)$. However, the chirp parameter α in general depends on the instantaneous signal power $p(t)$, as shown in Fig. 1 for different modulator types. For properly taking this dependence into account, we use an extended chirp model where we expand α as Taylor series, $\alpha(p/p_0) = \alpha_0 + \alpha_1 p/p_0 + \ldots + \alpha_K(p/p_0)^K$ (p_0 denotes the peak power). This yields, for the phase of the optical signal,

$$\phi(t)=\frac{\alpha_0}{2}\ln\left(\frac{p(t)}{p_0}\right)+\frac{1}{2}\cdot\sum_{k=1}^{K}\frac{\alpha_k}{k}\left(\frac{p(t)}{p_0}\right)^k. \qquad (1)$$

Figure 2(a) shows the simulated penalty in receiver sensitivity (in *dB* relative to the quantum limit) as a function of both the optical and electrical receiver bandwidth (scaled to data rate R) for chirp-free NRZ transmission.[4] For an input signal chirped by the InP/GaInAsP Mach-Zehnder modulator of Fig. 1, the contour lines of the sensitivity penalty are heavily modified (see Fig.2(b)). Maximum sensitivity, as indicated by

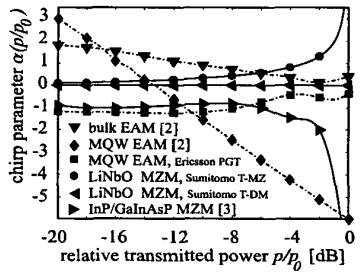

CThL50 Fig. 1. Chirp parameter α as function of transmitted power for different electroabsorption and Mach-Zehnder modulator types (own measurements and[2,3]).

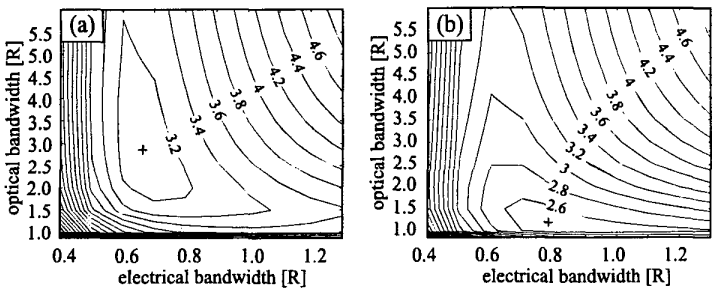

CThL50 Fig. 2. Receiver sensitivity penalty [*dB*] relative to the quantum limit as function of both electrical and optical bandwidth (normalized to data rate R) for (a) **chirp-free NRZ** transmission and for (b) **chirped NRZ signals** using modulator type "p" of Fig. 1.

the cross, is now obtained for different receiver bandwidths. Also, receiver sensitivity is improved, which is explained as follows: Chirp causes variations of the carrier frequency, especially during power transitions. In combination with narrow optical filtering, already low chirp may shift—during the edges of NRZ signals—a part of the signal energy out of the filter passband, resulting in pulse shortening for NRZ coding. By exploiting this reduction of intersymbol-interference (ISI), the receiver sensitivity can be improved by up to 1.7*dB* despite reduction of the received signal power. The optimum optical (electrical) bandwidth varies in the range of $1R \ldots 3R$ ($0.6R \ldots 1R$) for chirped signals obtained with the modulators of Fig. 1.

In the case of RZ reception, ISI plays a minor role, but chirp manifests itself as spectral broadening which can deteriorate the sensitivity up to 3*dB* and more, compared to chirp-free transmission. By optimizing the receiver with regard to chirp, the maximum penalty can be kept typically as low as 1.5*dB*, requiring broader optical filters in the range of $3R \ldots 10.5R$.

Our measurements performed with a dual-drive Mach-Zehnder modulator with adjustable chirp agree well with the simulation results.

References

1. N. Suzuki, Y. Hirayama, "Comparison of Effective α Parameters for Multiquantum-Well Electroabsorption Modulators", IEEE Photonics Techn. Lett., vol. 7, pp. 1007–1009, September 1995.
2. John C. Cartledge, Benny Christensen, "Optimum Operating Points for Electroabsorption Modulators in 10 Gb/s Transmission Systems Using Nondispersion Shifted Fiber", IEEE J. Lightwave Techn., vol. 16, pp. 349–357, March 1998.
3. John. C. Cartledge, "InP/GaInAsP phase-shifted Mach-Zehnder modulator for wavelength-independent performance in 10 Gbit/s transmission over dispersive fiber", OFC '97 Technical Digest, pp. 11–12, 1997.
4. Peter J. Winzer, Martin Pfennigbauer, Martin M. Strasser, Walter R. Leeb, "Optimum filter bandwidth for optically preamplified (N)RZ receivers", submitted to IEEE J. Lightwave Techn.

CThL51 **1:00 pm**

Bi-directional coupling in nonlinear waveguides for absolute timing determination

E.S. Awad, C.J.K. Richardson, P.S. Cho, N. Moulton, J. Goldhar, *Laboratory for Physical Sciences & Department of Electrical and Computer Engineering, University of Maryland College Park, MD, 20742; Email: esawad@ieee.org*

Future broadband optical networks will work at bit rates exceeding 100GHz through time-division multiplexing and wavelength-division multiplexing. For signal recovery a high-speed clock recovery or sub-clock recovery scheme is required. For 3R signal regeneration the recovered clock is needed for retiming of the optical signal. It is conventional to use a nonlinearity with a fast recovery time to determine temporal coincidence such as four wave mixing in a semiconductor optical amplifier,[1] or saturable absorption in an injection locked laser.[2] Schemes based on devices with slow nonlinear recovery times, such as an electroabsorption modulator, have been realized by applying an external electrical modulation.[3] The optical arrangement presented here monitors the difference between the nonlinear transmission of two pulses counter-propagating through a slow nonlinear medium, thus rapidly providing sufficient information to immediately determine the absolute timing error.

The arrival time between two counter-propagating picosecond laser pulses at a semiconductor nonlinear medium is absolutely determined by comparing both outputs of the non-linear device. Transient transmission fluctuations of the nonlinear waveguide occur because of saturation effects caused by the leading pulse. The experimental setup is shown in Fig. 1.

The setup shown in Fig. 1 uses two optical clocks built around mode-locked lasers operating at approximately 10GHz which are injected into the nonlinear device from opposite sides. The average optical transmission from each arm is detected with a balanced photodetector.

The behavior of an electroabsorption modulator (EAM) and a semiconductor optical amplifier (SOA) as nonlinear devices has been investigated. The features of the bipolar signal of the balanced photodetector depend on the carrier relaxation processes of the semiconductor nonlinear device. With the setup shown in Fig. 1, devices that exhibit a wide range of recovery time can be successfully used. These features can be observed by synchronizing the two oscillators and driving the mode-locked lasers at frequencies that differ by a fixed amount. A comparison of the signal for an EAM and a SOA are shown in Fig. 2 for a difference frequency of 10MHz.

A direct application of this optical system is to use the electrical signal of the balanced photodetector as an error signal in an optoelectronic phase-lock loop. This system is shown in Fig. 1, where the error signal is used to adjust a voltage-controlled oscillator (VCO) that drives one of the mode-locked lasers. Fig. 3 shows the averaged pulse trains of both optical clocks on a sampling oscilloscope that are detected by high speed photodetectors.

When the control input to the VCO is disconnected the pulse trains are not locked together. Therefore, the averaged signal shown in the top graph of Fig. 3 shows only one pulse train. Tim-

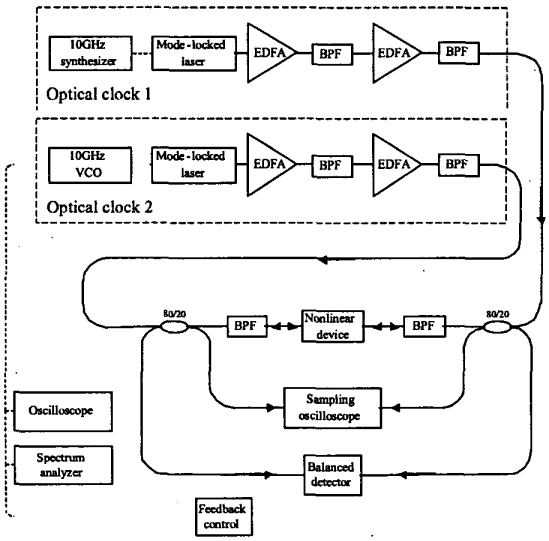

CThL51 Fig. 1. Schematic diagram of bi-directional nonlinear timing system for clock locking. Solid lines indicate optical connections, while dashed lines represent electrical connections.